



Plant protease, though often identified as a biological enzyme, can also be detected through its functional impact on protein degradation (Gurumallesh *et al.*, 2019). In SDS-PAGE tests, protease activity is evident from the breakdown of large protein molecules (e.g., myosin) into smaller peptides, visible as distinct bands with lower molecular weights. This indicates effective protein hydrolysis (Sujitha & Shanthi, 2023). Similarly, SEM analysis reveals structural changes in the extracellular matrix, such as damage to the perimysium and endomysium in muscle tissues. The disruption of these connective tissue layers suggests the protease's role in breaking down complex protein structures, confirming its functional presence without requiring direct isolation of the enzyme (Lieber & Meyer, 2023).

From a review of research conducted between 2010 and 2023 (Fig.1), we identified 1321 papers focusing on *C. citratus*. Between 2010 and 2016, the majority of studies concentrated on analyzing its biochemical composition for biofilms, protease inhibitors, and spices. From 2017 to 2019, research increasingly focused on its use as an anti-fungal, anti-bacterial, and pharmacological agent. During the Covid-19 pandemic, from 2020 to 2023, its utilization expanded into the fields of antibiotics, virus resistance, and further into the food and cosmetics industries. However, we found no studies specifically addressing proteases in *C. citratus*. This represents a significant research gap, which we aim to address by examining the effectiveness of proteases in this plant.

To date, no research has specifically focused on the effectiveness of proteases in the stumps and leaves of *C. citratus*. Investigating the variations in proteolytic activity between these two parts is particularly intriguing, especially in relation to the presence and interaction of proteases and inhibitors. The current lack of detailed information on the effectiveness of proteases in specific parts of *C. citratus* presents an opportunity to delve into the functional differences and potential uses of these proteolytic enzymes.

While numerous studies have highlighted the biochemical potential of *C. citratus* (Lamien-meda & Franz, 2011; Majewska *et al.*, 2019; Oladeji *et al.*, 2019), there is a noticeable gap in research comparing the biochemical properties of the plant's stumps and leaves. Analyzing the presence of compounds such as aldehydes, ketones, alcohols, esters, and terpene hydrocarbons in these parts is a promising area for further study (Ekpenyong *et al.*, 2014). Understanding the correlation between these biochemical compounds and proteolytic activity is crucial, particularly in the context of essential oil extraction, as it may influence both enzymatic functionality and potential industrial applications. The objectives of this research are two-fold: (i) to analyze the biochemical composition, including aldehydes, ketones, alcohols, esters, and terpene hydrocarbons, in the stumps and leaves of *C. citratus*; and (ii) to test the effectiveness of protease enzymes. This will be done by examining protein degradation zones and assessing how protein degradation impacts the structure of the extracellular matrix (including muscle tissue, perimysium, endomysium, and collagen) in goat meat and beef. This research aims to bridge the knowledge gap and expand our understanding of the biochemical and functional properties of *C. citratus*.

## MATERIAL AND METHODS

The *C. citratus* plants used in this study were obtained from agricultural products in the Magetan-East Java, Indonesia. The samples were categorized into two distinct parts: the stump part (CCS), which refers to the white lower stem of the plant, and the leaf part (CCL). To ensure freshness and quality, goat meat and beef samples were procured directly from local slaughterhouses.

### Oil extraction

The samples of *C. citratus*, including both leaves and stumps, were dried at a temperature of 27 °C for one week, the leaves were specifically laid out on trays for this process. To extract the essential oil from these *C. citratus* samples, two distinct methods were utilized. The first method, hydrodistillation, involved extracting 500g of the sample for about 60 min. The second method, microwave-assisted extraction, required placing 500g of ground sample and 2 L of distilled water in a spherical flask. This mixture was then processed in a microwave oven at 70°C for 24 h to yield the oil. Essential oil extracted from both the leaves and stumps of *C. citratus* was then prepared for analysis. This process has been previously conducted by our team, albeit with different samples (Budianto *et al.*, 2023).

### Meat preparation

Referring to the method proposed by (Budianto *et al.*, 2023), meat samples, including both beef and goat meat, were prepared into thin slices of 5 cm x 5 cm x 1 mm. These slices were then evenly coated with *C. citratus* oil extract, using a 1:1 weight/weight ratio, and left for 60 min. To avoid changes from temperature, samples were placed in a controlled environment of 20-22°C temperature. Samples were then ready for analysis using SDS-PAGE (Sodium Dodecyl Sulfate-Polyacrylamide Gel Electrophoresis) and SEM (Scanning Electron Microscopy) tests. Additionally, control samples, which did not undergo any treatment, were also prepared for comparative purposes.

## Sodium Dodecyl Sulphate Polyacrylamide Gel Electrophoresis (SDS-PAGE)

The analysis of protein degradation was conducted using SDS-PAGE (Sodium Dodecyl Sulfate-Polyacrylamide Gel Electrophoresis) based on the procedure established by the Association of Official Analytical Chemists (Association of Official Analytical Chemists., 2016). This analytical technique involved the use of acrylamide gel electrophoresis, which comprised two layers: a top layer consisting of a 5% stacking gel, and a bottom layer made of a 10% separating gel.

## Scanning Electron Microscopy (SEM)

We had previously performed this procedure in our previous research (Budianto *et al.*, 2023). Meat structure was analyzed using SEM (ZEISS, tipe EVOMA 10). The profiles of the meat were displayed on the secondary electron detector (SE).

### Biochemical Analysis: Gas Chromatografi / Mass Spectrometry (GC-MS)

This analytical procedure, based on the method described by Lamien-Meda & Franz (2011), utilizes gas chromatography (GC) to analyze the constituents of the essential oil extracted from the plant parts used, employing a Shimadzu GC-2050 (Shimadzu Corporation, Japan). For this purpose, two µL of the hexane solution (diluted to 1/105 v/v) was injected into a gas chromatograph equipped with a Restek Rtx-5Sil MS column. The GC conditions were set as follows: an injector temperature of 250°C, operated in no-separation mode, a helium carrier gas flow rate of 1 mL/min, and an interface temperature also at 250°C. The temperature program was initiated at 55°C, followed by an increase of 1°C per min until reaching 150°C, and then a further increase of 5°C per min until it reached 250°C, where it was maintained for 5 min. The identification of constituents was carried out by comparing their retention times with those in the NIST literature references (Stein *et al.*, 2002). The relative concentrations (%) of the constituents were calculated based on the GC peak areas, without applying correction factors.

Additionally, the GCT Premier instrument (Gas Chromatography-Time of Flight Mass Spectrometry, GC-TOF MS) was used for Electron Ionization (EI) analysis under the following conditions: a source temperature of 200°C, electron energy set at 70 eV, and an emission current of 400 µa. All ions generated were directed into the analysis zone, with an integration time of 1 second for each measurement.

## RESULTS AND DISCUSSION

The proteolytic activity in essential oil from *C. citratus* can still be detected even if only oil extraction is performed. Many studies indicate that this oil exhibits proteolytic effects similar to those of protease enzymes, as evidenced by SDS-PAGE tests showing the degradation of proteins into smaller fragments. Additionally, SEM analysis reveals significant structural changes in the tissue, demonstrating protease activity. This suggests that, although the extraction process does not involve direct enzyme isolation, the resulting essential oil retains relevant proteolytic activity.

### SDS-PAGE

SDS-PAGE analysis was carried out to examine the protein profile and investigate the protein interactions of beef and goat meat after being coated with sample extracts, which results are presented in Fig. 2.

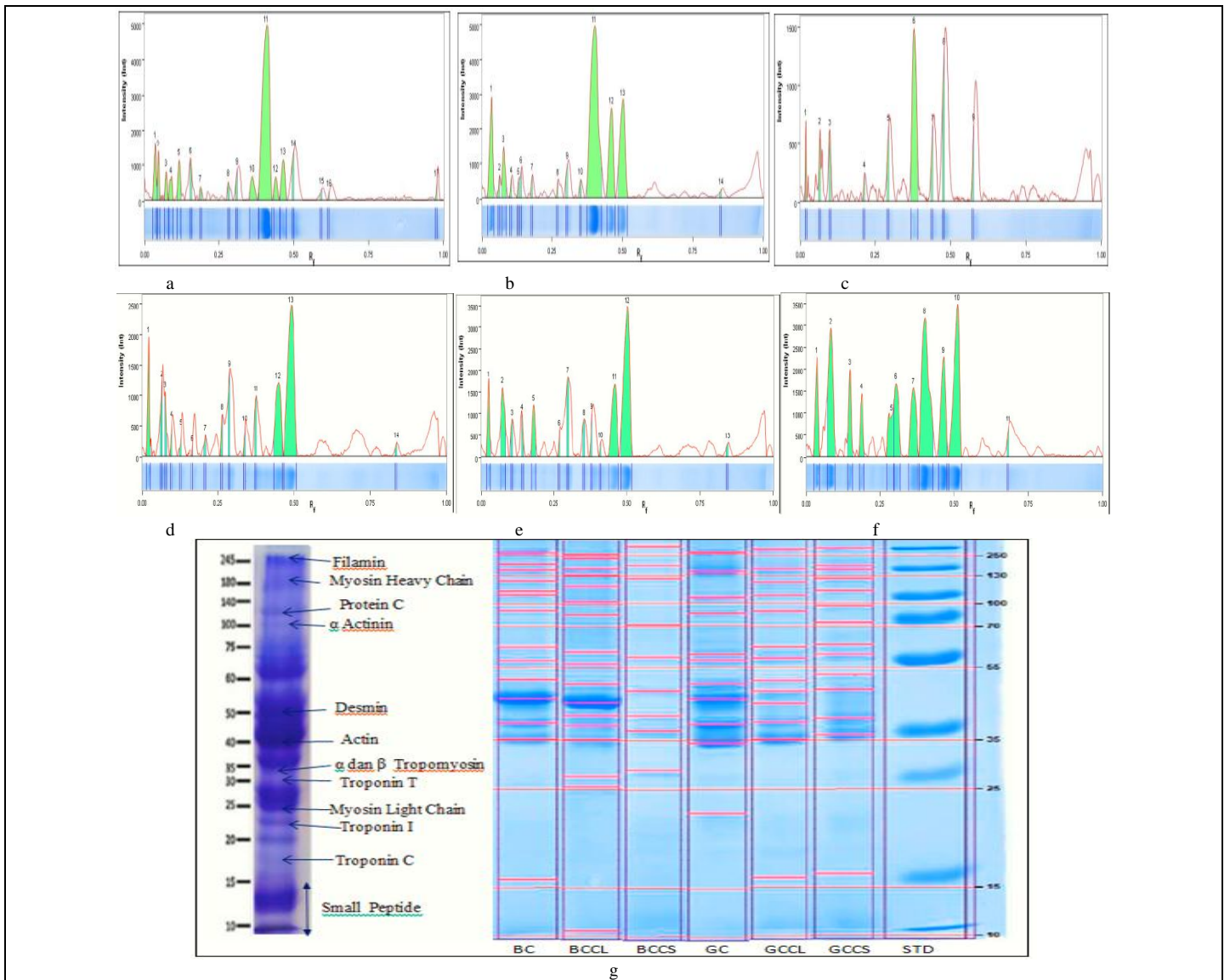


**Figure 2** Protein degradation in meat by *Cymbopogon citratus* protease. Path and Band analysis in control goat meat (a), GCCL (b), GCCS (c), control beef (d), BCCL (e), BCCS (f), protein degradation zone in goat and beef (g). **Note:** GC: Goat control; GCCL: Goat + *Cymbopogon citratus* leaf; GCCS: Goat + *Cymbopogon citratus* stump; BC: Beef control; BCCL: Beef+ *Cymbopogon citratus* leaf; BCCS: Beef+ *Cymbopogon citratus* stump; STD: standard.

**Goat Meat**

After electrophoresis, the GC sample exhibited 17 bands (Fig. 2a), the GCCL sample showed 14 bands (Fig. 2b), and the GCCS sample presented 9 bands (Fig. 2c). The molecular weights of the proteins detected in the GC sample were as follows: 10.5, 25.5, 27.3, 35.2, 38.5, 40.9, 44.3, 49.8, 56.3, 60.4, 84.7, 102.4, 118.2, 133.6, 165.4, 232.7, and 250 kDa.

In the GCCL samples, *C. citratus* protease effectively degraded proteins in the small peptide range (10-15 kDa), as evident from Fig. 2b and 2g. This is illustrated by the smallest detected molecular weight at band 14 (15.6 kDa). Partial degradation was observed in the myosin heavy chain (180-240 kDa), indicated by bands 1 and 2 (250, 188.4 kDa) in comparison to the control sample (GC), where they were found to be 250 and 232.7 kDa, respectively.

In the GCCS samples, the essential oil of *C. citratus* was capable of completely degrading proteins in the range of 10-28 kDa, encompassing small peptides, troponin C, troponin I, myosin light chain, and troponin T. As shown in Fig. 2c and 2g, the lowest molecular weight in these samples was observed in band 9 (28.5 kDa). Similar to the GCCL sample, light degradation was noted in the molecular weight range of 180-240 kDa. These results lend credence to the notion that degradation of the Troponin T region significantly influences the binding of actin and myosin (Cheng et al., 2021; Gagaoua et al., 2021) as well as  $\alpha$ ,  $\beta$  Tropomyosin (Budianto et al., 2023).

**Beef**

In the control sample (BC), electrophoresis revealed 14 bands (Fig. 2d), with molecular weights as follows: 250, 181.4, 158.1, 126.8, 112.9, 96.6, 74.6, 62.9, 59.5, 52.7, 48.0, 40.1, 36.1, and 10 kDa. Fig. 2g provides a comparative analysis

of the degradation zones in the BCCL and BCCS samples relative to the BC control.

In the BCCL samples, *C. citratus* protease effectively degraded proteins within the 10-15 kDa range, specifically small peptides. This is demonstrated in Fig. 2e and 2g, where the smallest molecular weight detected was in band 13 (15.8 kDa). There was also moderate degradation (indicated by a fading blue color) in the molecular weight range of 162.9 – 250 kDa, encompassing proteins such as myosin heavy chain and filamin.

The protease showed even broader degradation capabilities in the BCCS samples, targeting the 10-22 kDa range, which includes small peptides, troponin C, and troponin I. This is evident in Fig. 2f, where the lowest molecular weight band is 22.1 kDa, and in Fig. 2g, where a complete fading of the blue color is observed compared to the BC sample. Additionally, complete degradation was noted in the molecular weight range of 143 – 250 kDa, affecting proteins like myosin heavy chain and filamin.

The protease activity in *C. citratus* leaves was observed to specifically target and degrade goat meat proteins within a narrow molecular weight range of 10-15 kDa, corresponding to small peptides. A similar pattern of activity was noted in beef, with protease affecting the same molecular weight range. Despite its limited scope, this finding substantiates the presence of protease in *C. citratus* leaves and supports the hypothesis of abundant protease inhibitors in the leaves, aligning with previous studies on its inhibitory activity (Jagdale et al., 2015; Waghulde et al., 2021). Small peptides, being proteins with the lowest molecular weights (10-17.5 kDa), are particularly susceptible to degradation by proteases, even at low levels, as demonstrated in our earlier research (Budianto et al., 2023) and corroborated by other studies (Gagaoua et al., 2021; Hafid et al., 2020).

When comparing the effectiveness of proteases, those in *C. citratus* stumps were found to be more effective than those in the leaves. Although the degradation did not extend to the Desmin region, which is crucially linked to the Z line or midline

(Koochmarai & Shackelford, 1991) and is an indicator of meat tenderness (Wheeler & Koochmarai, 1999), it did affect the myosin heavy chain and filamin areas in beef. It is important to note that the extent of degradation in these areas might also be influenced by factors related to meat slaughtering and storage (Latorre et al., 2018). While the efficacy of *C. citratus* protease may not match that of proteases found in papain (Latorre et al., 2018), bromelain (Nanda et al., 2020), or metalloprotease (Minaev & Makhova, 2019), this research successfully demonstrates the proteolytic capability of *C. citratus*.

**The influence of *C. citratus* on extracellular matrix structure**

In meat connective tissue, we primarily observe muscle tissue, endomysium, perimysium, and collagen. Muscle fibers, located within muscle cells, are enveloped by the endomysium, a thin layer of connective tissue. The perimysium, a thicker layer of connective tissue, encases a bundle of muscle fibers along with the endomysium. Collectively, these elements (muscle fibers, endomysium, and perimysium) form what are known as muscle bundles. Collagen, a key protein in connective tissue, predominantly forms the extracellular matrix.

Our research indicates that *C. citratus* protease can effectively reduce intramuscular isometric tension, despite being present in only small quantities in the leaves. Analysis of both leaf and stump samples revealed their ability to efficiently separate myofibers from the perimysium. Within the proteoglycan matrix, the perimysium is observed to intersect with collagen fibers in a neatly arranged pattern (Turrina et al., 2013). The fibers of the perimysium typically form waves parallel and at symmetrical angles to muscle fibers (Aristizabal et al., 2014; Turrina et al., 2013). Damage to the perimysium often results in deeper cracks in the endomysium (Du et al., 2021). In our study, the protease from *C. citratus* was found to cause small and deep cracks indicative of damage to both the perimysium and endomysium

**Goat meat**

In GC samples (control), the meat connective tissue primarily consists of muscle tissue and collagen (Fig. 3a). The integrity of the tissue is largely intact, exhibiting tightness without significant tearing, except for visible knife marks. The robust and cohesive nature of the meat imparts a tough and chewy texture. However, the application of *C. citratus* leaf protease significantly alters the meat's connective tissue (Fig. 3b). Here, the perimysium becomes more prominent, characterized by small tears or cracks, while the endomysium is also present but distributed unevenly. Although collagen remains visible, it no longer dominates the tissue. This results in a reduction in the meat's hardness and ductility compared to the GC samples.

In the GCCS samples, endomysium tissue is predominant (Fig. 3c) and uniformly distributed throughout. The presence of wide and deep tears indicates the breakdown of perimysium bonds, thereby making the endomysium fibers more visible. Although perimysium still appears in certain areas as small cracks, and muscle tissue and collagen are also present, the dominance of endomysium significantly contributes to the meat's tenderness. Of the three samples, the effect of *C. citratus* protease is most pronounced in the GCCS samples.

The impact of *C. citratus* protease on the connective tissue of goat meat is significant. In control samples, a high prevalence of muscle and collagen tissue was noted, reflecting the meat's strength and resilience. However, upon treatment with the protease, the leaves of *C. citratus* were observed to alter the intramuscular isometrics, leading to a dominance of perimysium in the meat samples and visible endomysium at various points. Conversely, proteases from *C. citratus* stumps exhibited a more pronounced degradation effect, characterized by a predominance of endomysium and visibly elongated muscle fibers. These findings also demonstrate that damage to endomysial tissue results in muscle fibers becoming straight and elongated, consequently influencing the straightness of collagen fibers (Du et al., 2021), in contrast to the typically wavy appearance of undegraded collagen (Gathercole & Keller, 1991).

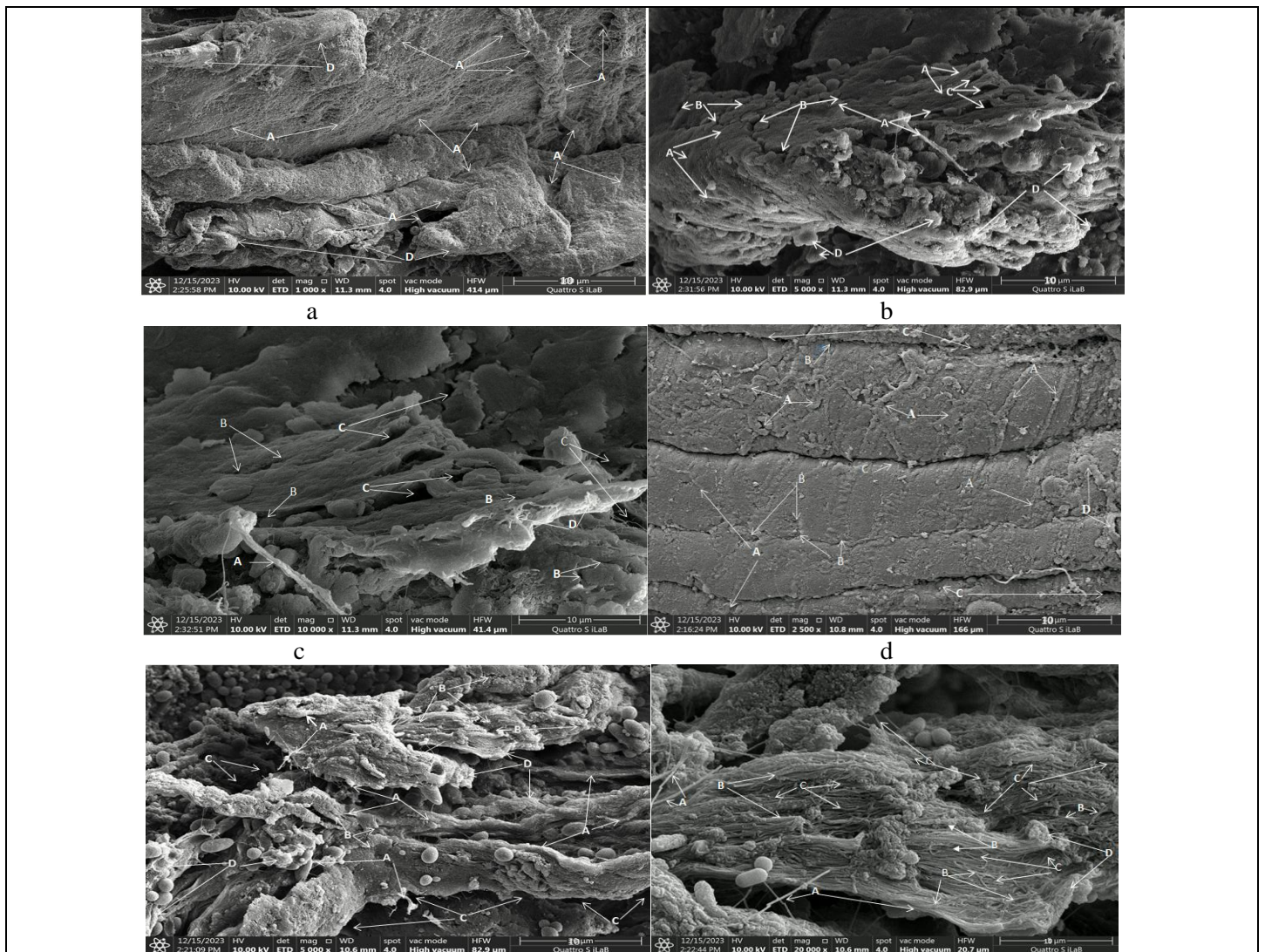


**Figure 3** The effect of *Cymbopogon citratus* protease on the extracellular matrix structure. Control goat meat (a), GCCL (b), GCCS (c), Control Beef/ BC (d), BCCL (e), and BCCS (f). **Note:** Muscle tissue (A), perimysium (B), endomysium (C), dan collagen (D)

Similar to the GC sample, the BC sample also exhibits comparable characteristics (Fig. 3d). The meat's surface is primarily composed of muscle tissue and collagen, with the perimysium visible at certain spots. The meat retains a tough and chewy character when consumed.

In the BCCL sample, numerous tears in the flesh are evident (Fig. 3e). The perimysium is still more prominent compared to the endomysium, muscle tissue, and collagen. This alteration results in the meat losing its toughness and exhibiting a softer texture. Despite the dominance of perimysium, it does not prominently display the muscle fibers that are typically encased within the endomysium.

The application of *C. citratus* protease in the BCCS sample effectively reveals muscle fibers located within the endomysium (Fig. 3f). The endomysium is dominant throughout, with noticeable presence of perimysium as well. Muscle tissue and collagen are still visible at certain points. Compared to the BC and BCCL samples, the texture of the meat in the BCCS sample is notably softer.

The proteolytic activity of *C. citratus* stump protease on beef appears to be more effective than that of *C. citratus* leaf protease. The stump protease causes a notable elongation and separation of muscle fibers, with the endomysium being predominantly affected over the perimysium. As a result, the collagen fibers appear elongated and lose their typical wavy structure. In contrast, beef treated with *C. citratus* leaf protease shows a dominant perimysium, though the endomysium is visible at several points. The collagen fibers in this case retain a wavy form, but there are instances where the fibers become straight and elongated. While the hierarchical relationships between endomysial and perimysial structures in muscle

tissue are not universally established (Cheng et al., 2021), the degradation effect does not alter the functional role of collagen fibers in connecting the perimysium and endomysium (Light & Champion, 1984).

**Biochemical composition**

The biochemical analysis of *C. citratus* essential oil focused on identifying aldehydes, ketones, alcohols, esters, and hydrocarbon terpenes. This study compared the biochemical composition of the plant's corms and leaves, with the findings detailed in Tables 1 and 2.

In the corms of *C. citratus*, aldehyde and ketone compounds were notably prevalent, constituting 88.57% of the detected compounds, whereas in the leaves, these compounds were present at a slightly lower percentage of 81.24%. Geraniol and neral were identified as the dominant compounds in this category. However, certain compounds, specifically Camphor and Isogeraniol, were absent in both corm and leaf samples. Trans-Chrysanthamal was detected in both, but only in minimal amounts (0.14-0.15%). These findings align with previous research, albeit reported in a review format (Majewska et al., 2019), which does not specify the part of *C. citratus* studied.

Regarding alcohol group compounds, the leaves of *C. citratus* exhibited a higher percentage (55.93%) compared to the corms, which had 45.84%. Among these, geraniol was the most dominant. Both corm and leaf samples showed the absence of several compounds, namely  $\gamma$ -eucalyptol, trans-farnesol, isoborneol, and trans-verbenol. Detailed results of these findings are presented in Table 1.

**Table 1** The composition of aldehydes, ketones and alcohol in *Cymbopogon citratus*

Aldehydes and ketones				
Compound	Kovats RI <sup>1</sup>	Stump (%)	Leaf (%)	Classification
Camphor	1146	nd	nd	Monoterpenoid ketone
2-Caren-10-al	1711	0,23	0,31	Monoterpenoid aldehyde
(+)-Carvotanacetone	1213	0,37	0,34	Monoterpenoid ketone
trans-Chrysanthamal	1451	0,15	0,14	Monoterpenoid aldehyde
Citronellal	1134	0,36	12,77	Monoterpenoid aldehyde
Geraniol	1244	48,24	41,45	Monoterpenoid aldehyde
Isogeraniol	1237	nd	nd	Monoterpenoid aldehyde
Lauraldehyde	1224	0,34	0,3	Monoterpenoid aldehyde
Neral	1211	37,42	24,57	Monoterpenoid aldehyde
Piperitone	1282	0,88	0,89	Monoterpenoid ketone
2-Undecanone	1549	0,58	0,47	Aliphatic ketone
<b>Total (%)</b>		<b>88,57</b>	<b>81,24</b>	
Alcohols				
Borneol	1642	4,68	5,01	Monoterpenoid alcohol
$\alpha$ -Cadinol	1652	0,35	0,45	Sesquiterpenoid alcohol
Carotol	1594	0,32	0,34	Sesquiterpenoid alcohol
$\beta$ -Citronellol	1435	2,83	3,03	Monoterpenoid alcohol
Cubenol	1645	0,23	0,86	Sesquiterpenoid alcohol
Elemol	1547	1,32	2,43	Sesquiterpenoid alcohol
$\alpha$ -Eudesmol	1649	0,35	0,56	Sesquiterpenoid alcohol
$\beta$ -Eudesmol	1630	0,35	0,48	Sesquiterpenoid alcohol
$\gamma$ -Eudesmol	1616	0,36	0,51	Sesquiterpenoid alcohol
$\gamma$ -Eucalyptol	1039	nd	nd	Monoterpenoid ether
trans-Farnesol	1705	nd	nd	Sesquiterpenoid alcohol
Geraniol	1276	21,86	24,32	Monoterpenoid alcohol
Globulol	1576	1,02	1,41	Sesquiterpenoid alcohol
Hinesol	1638	0,67	0,92	Sesquiterpenoid alcohol
Isoborneol	1156	nd	nd	Monoterpenoid alcohol
Isopulegol	1728	0,21	0,36	Monoterpenoid alcohol
Linalool	1082	0,67	0,73	Monoterpenoid alcohol
3-Methylcyclohexanol	929	0,23	0,82	Aliphatic alcohol
E-Methyleugenol	1401	0,21	0,34	Phenylpropanoid ether
Methylisoeugenol	1461	7,4	9,3	Phenylpropanoid ether
Nerol	1228	0,21	0,42	Monoterpenoid alcohol
Terpinen-4-ol	1178	2,23	3,21	Monoterpenoid alcohol
cis-Verbenol	1244	0,34	0,43	Monoterpenoid alcohol
trans-Verbenol	1150	nd	nd	Monoterpenoid alcohol
<b>Total (%)</b>		<b>45,84</b>	<b>55,93</b>	

The ester compounds in *C. citratus* exhibited a varied composition between the leaves and tubers. The leaves showed a higher percentage of ester compounds compared to the tubers. Among these, Citronellylisobutyrate was the most prominent, but the composition was relatively balanced across all detected ester compounds. Notably, geranyl butyrate and geranylformate were absent in both the tubers and leaves.

In this study, the chord diagram serves to visualize the relationships and interactions between biochemical components, such as aldehydes, ketones, alcohols, esters, and terpene hydrocarbons, present in *C. citratus*. This diagram

helps clarify the patterns of association among these compounds, making it easier to analyze how they interact or are distributed. Thus, the chord diagram complements the composition tables (Table 1 and Table 2) by providing an intuitive visual representation, facilitating the identification of relationships that may be less apparent in numerical data alone.

The composition of aldehydes, ketones, and alcohols in *C. citratus* shows slight differences between the leaf and stump parts, with the leaf having a slightly wider band (137.17) compared to the stump (134.41). Both parts are dominated by

geranial, geraniol, and neral. However, a notable difference is observed in the leaf, where citronellal dominates, distinguishing it from the stump (Fig. 4a).

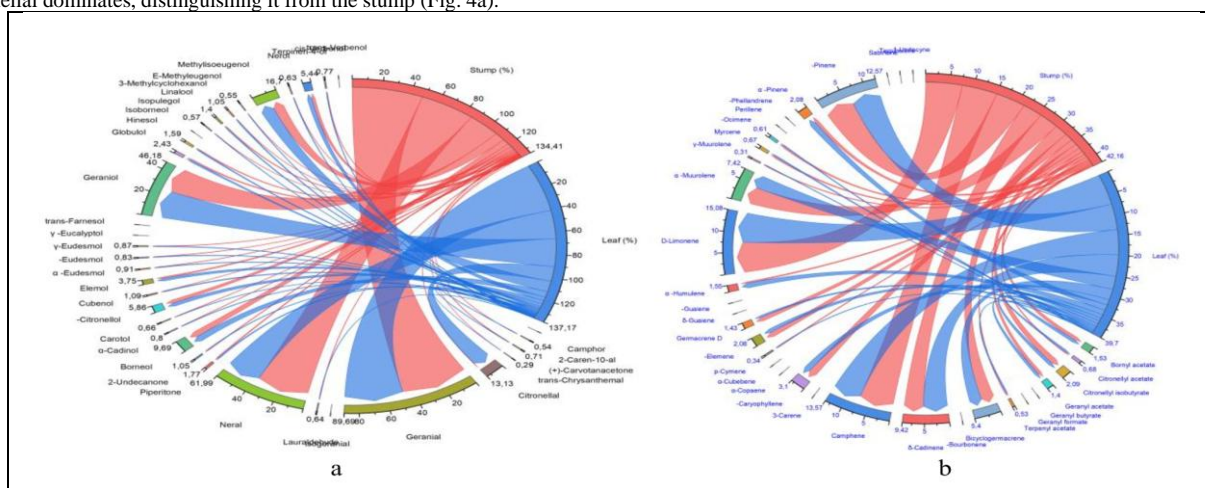


Figure 4 Biochemical Composition of *C. citratus*: Aldehydes, Ketones, and Alcohols (a); Esters and Terpene Hydrocarbons (b).

The composition of esters and terpene hydrocarbons in *C. citratus* shows that the stump has a wider band (42.16) compared to the leaf (39.7). The difference is particularly evident in the stump, where  $\alpha$ -Muurolene and camphene are more prominent, distinguishing it from the leaf (Fig 4b). The analysis of terpene hydrocarbon compounds revealed a fairly uniform distribution between the tubers and leaves, with a slightly higher presence in the

tubers. Camphene, D-Limonene, and -Pinene were the dominant compounds in both samples. However, several compounds were not detected in either the tubers or leaves. These include  $\beta$ -Bourbonene, 3-Carene,  $\alpha$ -Copaene,  $\alpha$ -Cubebene,  $\delta$ -Guaiene,  $\beta$ -Guaiene, Perillene,  $\beta$ -Phellandrene, Sabinene, Terpinolene, and 1-Undecyne. Comprehensive results of these findings are detailed in Table 2.

Table 2 Composition of Esters and Terpene Hydrocarbons in *Cymbopogon citratus*

Esters			
Compound	Kovats RI <sup>1</sup>	Stump (%)	Leaf (%)
Bornyl acetate	1285	0,81	0,72
Citronellyl acetate	1354	0,23	0,45
Citronellyl isobutyrate	1482	1,34	0,75
Geranyl acetate	1383	0,71	0,69
Geranyl butyrate	1562	nd	nd
Geranyl formate	1300	nd	nd
Terpenyl acetate	1352	0,24	0,29
<b>Total (%)</b>		<b>2,62</b>	<b>2,9</b>
Hydrocarbon terpenes			
Bicyclogermacrene	1494	2,8	2,6
$\beta$ -Bourbonene	1380	nd	nd
$\delta$ -Cadinene	1513	4,21	5,21
Camphene	953	7,45	6,12
3-Carene	1011	nd	nd
$\beta$ -Caryophyllene	1467	1,76	1,34
$\alpha$ -Copaene	1391	nd	nd
$\alpha$ -Cubebene	1345	nd	nd
p-Cymene	1033	0,21	0,13
$\beta$ -Elemene	1393	1,21	0,87
Germacrene D	1499	0,98	0,45
$\delta$ -Guaiene	1511	nd	nd
$\beta$ -Guaiene	1490	nd	nd
$\alpha$ -Humulene	1710	0,34	1,21
D-Limonene	1039	7,65	7,43
$\alpha$ -Muurolene	1499	4,21	3,21
$\gamma$ -Muurolene	1477	0,18	0,13
Myrcene	994	0,35	0,32
$\beta$ -Ocimene	1029	0,4	0,21
Perillene	1109	nd	nd
$\beta$ -Phellandrene	1005	nd	nd
$\alpha$ -Pinene	933	0,74	1,34
$\beta$ -Pinene	981	6,34	6,23
Sabinene	976	nd	nd
Terpinolene	1096	nd	nd
1-Undecyne	1112	nd	nd
<b>Total (%)</b>		<b>38,83</b>	<b>36,8</b>

The study by Farhang et al. (2013) revealed that *C. citratus* oil from Iran contains citral (30.95%, aldehyde), limonene (5.83%, monoterpene), and caryophyllene (3.44%, sesquiterpene) as major components. Minor compounds include methyheptenone (1.2%, ketone) and naphthalene (0.79%, aromatic hydrocarbon).

Phytochemical analysis revealed that *C. citratus* from Saudi Arabia is dominated by  $\beta$ -eudesmol (45%) and elemol (41%) (Halabi & Sheikh, 2014). In Nigeria, citral (33.7%, 26.5%, 25.3%) was the main component (Kasali et al., 2001), while

in Belgium, 23 (57.46%) and citral diethylacetal (24.68%) were prominent (Katsukawa et al., 2010).

The significance and limitation of this study

This study effectively highlights the proteolytic activity present in *C. citratus* essential oil, even with minimal extraction procedures. One of the key strengths of this research is the detection of proteolytic effects akin to protease enzymes, as demonstrated by SDS-PAGE, which shows protein degradation into smaller

fragments. Additionally, SEM analysis reveals structural changes in tissues, supporting the notion of protease activity. This suggests that the proteolytic capacity remains intact, despite the absence of direct enzyme isolation in the extraction process. These findings align with other studies where proteases influence the texture and structure of meat products, making it a promising candidate for food industry applications.

A notable limitation of the study is the lack of direct enzyme isolation, making it challenging to quantitatively assess or compare the proteolytic activity of *C. citratus* against better-known proteases, such as papain or bromelain. Furthermore, the variation in protease activity observed across different tissues and meat types indicates a need for further research to fully understand the enzyme's specificity and potential applications.

The significance of this study lies in its potential to identify a novel, renewable source of protease from *C. citratus*, a plant that has not been extensively studied for such applications. These findings open opportunities for further exploration of the biochemical composition of *C. citratus* essential oil and its application in industries requiring natural proteolytic agents. Future research should focus on isolating and characterizing specific protease and inhibitor compounds to enhance understanding and optimize its industrial applications in the food sector. Additionally, while this study highlights the proteolytic activity of *C. citratus*, its impact on the aroma of the evaluated meat was not the primary focus. Given that *C. citratus* possesses distinct organoleptic properties, its potential influence on the sensory characteristics of the final product should be considered in future studies.

## CONCLUSION

In terms of their chemical composition, *C. citratus* stump exhibit a higher concentration of aldehydes and ketones (88.57%) compared to the leaves (81.24%), with geraniol and neral being the most prevalent compounds. Notably, Camphor and Isogeraniol were absent, while trans-Chrysanthamal was detected in low quantities (0.14-0.15%). Regarding alcohol compounds, the leaves of *C. citratus* contained a higher percentage (55.93%) than those from the weevil (45.84%), with geraniol as the dominant component. Other compounds, such as  $\gamma$ -eucalyptol, trans-farnesol, isoborneol, and trans-verbenol, were not found in the samples. The results for ester compounds were relatively similar between the two parts of the plant, with the stump at 2.62% and the leaf at 2.9%.

The protease activity in *C. citratus* leaves demonstrates its capacity for degrading goat and beef protein within a narrow molecular weight range of 10-15 kDa. Conversely, the tubers showed a broader degradation spectrum in goat meat, affecting proteins in the 10-28 kDa range (including small peptide, troponin C, troponin I, myosin light chain, and troponin T). In beef, the protease from *C. citratus* was effective over a wider range: 10-22 kDa (targeting small peptide, troponin C, and troponin I) and 143 – 250 kDa (affecting myosin heavy chain, filamin).

The protease derived from *C. citratus* has a substantial impact on meat connective tissue. Its ability to degrade collagen and muscle tissue is evident, with tuber-derived proteases leading to a predominance of endomysium, while leaf-derived proteases result in a more perimysium-dominant structure in both goat and beef meat samples.

**Acknowledgments:** The authors would like to thank Institute of Science and Technology al-Kamal for the laboratory facilities provided in support of this research.

## REFERENCES

Adamczyk, B., Godlewski, M., Zimny, J., & Zimny, A. (2008). Wheat (*Triticum aestivum*) seedlings secrete proteases from the roots and, after protein addition, grow well on medium without inorganic nitrogen. *Plant Biology*, 10(6), 718–724. <https://doi.org/10.1111/j.1438-8677.2008.00079.x>

Adetobi, E. T., Akinsuyi, S. O., Ahmed, O. A., Folajimi, E. O., & Babalola, B. A. (2022). In silico Evaluation of the Inhibitory Potential of Cymbopogonol from Cymbopogon citratus Towards Falcipain-2 (FP2) Cysteine Protease of Plasmodium falciparum. *Tropical Journal of Natural Product Research*, 6(10).

Aristizabal, S., Amador, C., Qiang, B., Kinnick, R. R., Nenadic, I. Z., Greenleaf, J. F., & Urban, M. W. (2014). Shear wave vibrometry evaluation in transverse isotropic tissue mimicking phantoms and skeletal muscle. *Physics in Medicine & Biology*, 59(24), 7735. <https://doi.org/10.1088/0031-9155/59/24/7735>

Association of Official Analytical Chemists. (2016). Official methods of analysis of AOAC International (20th ed.). *AOAC International*.

Budianto, B., Arifin, M. J., Naryani, N., Sukmawati, E., Suwaji, S., Wibowo, T. H. M., Luviana, S. V., & Putri, L. D. V. (2023). Plant proteases and anti-bacterial substances in *Allium sativum* L. varieties. *Foods and Raw Materials*, 12(2), 240–248. <https://doi.org/10.21603/2308-4057-2024-2-606>

Cheng, Y., Jiang, X., Xue, Y., Qi, F., & Dai, Z. (2021). Effect of three different proteases on horsemeat tenderness during postmortem aging. *Journal of Food Science and Technology*, 58(7), 2528–2537. <https://doi.org/10.1007/s13197-020-04759-x>

Du, X., Li, H., Nuerjiang, M., Shi, S., Kong, B., Liu, Q., & Xia, X. (2021). Application of ultrasound treatment in chicken gizzards tenderization: Effects on

muscle fiber and connective tissue. *Ultrasonics Sonochemistry*, 79, 105786. <https://doi.org/10.1016/j.ultsonch.2021.105786>

Ekpenyong, C. E., Akpan, E. E., & Daniel, N. E. (2014). Phytochemical Constituents, Therapeutic Applications and Toxicological Profile of Cymbopogon citratus Stapf (DC) Leaf Extract. *Journal of Pharmacognosy and Phytochemistry*, 3(1), 133-141.

Farhang, V., Amini, J., Javadi, T., Nazemi, J., & Ebadollahi, A. (2013). Chemical composition and antifungal activity of essential oil of Cymbopogon citratus (DC.) Stapf. against three Phytophthora species. *Greener J Biol Sci*, 3, 292–298. <http://doi.org/10.15580/GJBS.2013.8.240913861>

Gagaoua, M., Dib, A. L., Lakhdera, N., Lamri, M., Botineştean, C., & Lorenzo, J. M. (2021). Artificial meat tenderization using plant cysteine proteases. *Current Opinion in Food Science*, 38, 177–188. <https://doi.org/10.1016/j.cofs.2020.12.002>

Gathercole, L. J., & Keller, A. (1991). Crimp morphology in the fibre-forming collagens. *Matrix*, 11(3), 214–234. [https://doi.org/10.1016/S0934-8832\(11\)80161-7](https://doi.org/10.1016/S0934-8832(11)80161-7)

Gurumalles, P., Alagu, K., Ramakrishnan, B., & Muthusamy, S. (2019). A systematic reconsideration on proteases. *International Journal of Biological Macromolecules*, 128, 254–267. <https://doi.org/10.1016/j.ijbiomac.2019.01.081>

Hafid, K., John, J., Sayah, T. M., Dominguez, R., Becila, S., Lamri, M., Dib, A. L., Lorenzo, J. M., & Gagaoua, M. (2020). One-step recovery of latex papain from Carica papaya using three phase partitioning and its use as milk-clotting and meat-tenderizing agent. *International Journal of Biological Macromolecules*, 146, 798–810. <https://doi.org/10.1016/j.ijbiomac.2019.10.048>

Halabi, M. F., & Sheikh, B. Y. (2014). Anti-Proliferative Effect and Phytochemical Analysis of Cymbopogon citratus Extract. *BioMed Research International*, 2014(1), 906239. <https://doi.org/10.1155/2014/906239>

Jagdale, A. D., Kamble, S. P., Nalawade, M. L., & Arvindekar, A. U. (2015). Citronellol: A potential antioxidant and aldose reductase inhibitor from Cymbopogon citratus. *Int. J. Pharm. Pharm. Sci*, 7, 203-209.

Kasali, A. A., Oyedeji, A. O., & Ashilokun, A. O. (2001). Volatile leaf oil constituents of Cymbopogon citratus (DC) Stapf. *Flavour and Fragrance Journal*, 16(5), 377–378. <https://doi.org/10.1002/ffj.1019>

Katsukawa, M., Nakata, R., Takizawa, Y., Hori, K., Takahashi, S., & Inoue, H. (2010). Citral, a component of lemongrass oil, activates PPAR $\alpha$  and  $\gamma$  and suppresses COX-2 expression. *Biochimica et Biophysica Acta (BBA) - Molecular and Cell Biology of Lipids*, 1801(11), 1214–1220. <https://doi.org/10.1016/j.bbalip.2010.07.004>

Koohmaria, M., & Shackelford, S. D. (1991). Effect of calcium chloride infusion on the tenderness of lambs fed a  $\beta$ -adrenergic agonist. *Journal of Animal Science*, 69(6), 2463–2471. <https://doi.org/10.2527/1991.6962463x>

Lamien-meda, A., & Franz, C. (2011). Chemical composition and antimicrobial activity of Cymbopogon citratus and Cymbopogon giganteus essential oils alone and in combination. *18*, 1070–1074. <https://doi.org/10.1016/j.phymed.2011.05.009>

Latorre, M. E., Velázquez, D. E., & Purslow, P. P. (2018). The thermal shrinkage force in perimysium from different beef muscles is not affected by post-mortem ageing. *Meat Science*, 135, 109–114. <https://doi.org/10.1016/j.meatsci.2017.09.003>

Lieber, R. L., & Meyer, G. (2023). Structure-Function relationships in the skeletal muscle extracellular matrix. *Journal of Biomechanics*, 152, 111593. <https://doi.org/10.1016/j.jbiomech.2023.111593>

Light, N., & Champion, A. E. (1984). Characterization of muscle epimysium, perimysium and endomysium collagens. *Biochemical Journal*, 219(3), 1017–1026. <https://doi.org/10.1042/bj2191017>

Majewska, E., Kozłowska, M., Gruczynska-Sekowska, E., Kowalska, D., & Tarnowska, K. (2019). Lemongrass (*Cymbopogon citratus*) essential oil: Extraction, composition, bioactivity and uses for food preservation - A review. *Polish Journal of Food and Nutrition Sciences*, 69(4), 327–341. <https://doi.org/10.31883/pjfn/113152>

Minaev, M. Y., & Makhova, A. A. (2019). RECOMBINANT METALLOPROTEASE AS A PERSPECTIVE ENZYME FOR MEAT TENDERIZATION. *Potravinarstvo*, 13(1). <https://doi.org/10.5219/1087>

Mipeshwaree Devi A, Khedashwori Devi K, Premi Devi P, LakshmiPriyari Devi M, Das S. Metabolic engineering of plant secondary metabolites: prospects and its technological challenges. *Front Plant Sci*. 2023 May 12;14:1171154. <https://doi.org/10.3389/fpls.2023.1171154>

Nanda, R. F., Bahar, R., Syukri, D., Thu, N. N. A., & Kasim, A. (2020). A review: Application of bromelain enzymes in animal food products. *Andalasian International Journal of Agriculture and Natural Sciences (AIJANS)*, 1(01), 33–44. <https://doi.org/10.25077/aijans.v1.i01.33-44.2020>

Oladeji, O. S., Adelowo, F. E., Ayodele, D. T., & Odelade, K. A. (2019). Phytochemistry and pharmacological activities of Cymbopogon citratus: A review. *Scientific African*, 6, e00137. <https://doi.org/10.1016/j.sciaf.2019.e00137>

Reshi ZA, Ahmad W, Lukatkin AS, Javed SB. From Nature to Lab: A Review of Secondary Metabolite Biosynthetic Pathways, Environmental Influences, and In Vitro Approaches. *Metabolites*. 2023 Jul 28;13(8):895. <https://doi.org/10.3390/metabo13080895>

Rifaldi, F., Mumpuni, E., Kumala, S., Yantih, N., Aulena, D. N., & Nafisa, S. (2022). Molecular docking of Cymbopogon nardus (L.) rendle compounds as a

- protease inhibitor of SARS-CoV-2. *Int. J. Appl. Pharm*, 14, 112–115. <https://dx.doi.org/10.22159/ijap.2022.v14s3.24>
- Ryan, C. A. (1973). Proteolytic enzymes and their inhibitors in plants. *Annual Review of Plant Physiology*, 24(1), 173–196. <https://doi.org/10.1146/annurev.pp.24.060173.001133>
- Stein, S., Mirokhin, D., Tchekhovskoi, D., Mallard, G., Mikaia, A., Zaikin, V., & Sparkman, D. (2002). The NIST mass spectral search program for the NIST/EPA/NIH mass spectra library. *Gaithersburg, MD: Standard Reference Data Program of the National Institute of Standards and Technology*.
- Sujitha, P., & Shanthi, C. (2023). Importance of enzyme specificity and stability for the application of proteases in greener industrial processing- a review. *Journal of Cleaner Production*, 425, 138915. <https://doi.org/10.1016/j.jclepro.2023.138915>
- Sytar, O., & Hajjhashemi, S. (2024). Specific Secondary Metabolites of Medicinal Plants and Their Role in Stress Adaptation. *Plant Secondary Metabolites and Abiotic Stress*, 425–479. <https://doi.org/10.1002/9781394186457.ch15>
- Sytar, O., Olšovská, K. Plant-based proteins as a food source and plant growth biostimulants. *Discov Food* 4, 78 (2024). <https://doi.org/10.1007/s44187-024-00161-0>
- Turrina, A., Martínez-González, M. A., & Stecco, C. (2013). The muscular force transmission system: role of the intramuscular connective tissue. *Journal of Bodywork and Movement Therapies*, 17(1), 95–102. <https://doi.org/10.1016/j.jbmt.2012.06.001>
- Vágnerová, K., & Macura, J. (1974). Relationships between plant roots, proteolytic organisms and activity of protease. *Folia Microbiologica*, 19, 525–535. <https://doi.org/10.1007/BF02872920>
- Van Der Hoorn, R. A. L. (2008). Plant proteases: from phenotypes to molecular mechanisms. *Annu. Rev. Plant Biol.*, 59, 191–223. <https://doi.org/10.1146/annurev.arplant.59.032607.092835>
- Waghulde, S., Parmar, P., Mule, J., Pashte, D., Patil, B., Modhale, N., Gorde, N., Kharche, A., & Kale, M. (2021). Lead Finding from Plant *Cymbopogon Citratus* with Immunomodulator Potentials through in Silico Methods. In *Chemistry Proceedings* 3(1).. <https://doi.org/10.3390/ecsoc-24-08302>
- Wheeler, T. L., & Koohmaraie, M. (1999). The extent of proteolysis is independent of sarcomere length in lamb longissimus and psoas major. *Journal of Animal Science*, 77(9), 2444–2451. <https://doi.org/10.2527/1999.7792444x>